Heavy Quark Physics at SLD*

(Preliminary Results)

Eric Vella

Representing the SLD Collaboration†

Stanford Linear Accelerator Center
Stanford University, Stanford, CA 94309

* This work was supported by Department of Energy contracts: DE-FG02-91ER40676 (BU), DE-FG03-92ER40701 (CIT), DE-FG03-91ER40618 (UCSB), DE-FG03-92ER40689 (UCSC), DE-FG03-93ER40788 (CSU), DE-FG02-91ER40672 (Colorado), DE-FG02-91ER40677 (Illinois), DE-AC03-76SF00098 (LBL), DE-FG02-92ER40715 (Massachusetts), DE-AC02-76ER03069 (MIT), DE-FG06-85ER40224 (Oregon), DE-AC03-76SF00515 (SLAC), DE-FG05-91ER40627 (Tennessee), DE-AC02-76ER00881 (Wisconsin), DE-FG02-92ER40704 (Yale); National Science Foundation grants: PHY-91-13428 (UCSC), PHY-89-21320 (Columbia), PHY-92-04239 (Cincinnati), PHY-88-17930 (Rutgers), PHY-88-19316 (Vanderbilt), PHY-92-03212 (Washington); UK Science and Engineering Research Council (Brunel and RAL); Istituto Nazionale di Fisica Nucleare of Italy (Bologna, Ferrara, Frascati, Pisa, Padova, Perugia); Japan-US Cooperative Research Project on High Energy Physics (Nagoya, Tohoku).

©E. Vella 1994

Heavy Quark Physics at SLD

(Preliminary Results)

SLD Experiment

- Luminosity and Polarization
- Tracking and Calorimetry
- Vertex Detector

$R_b = \Gamma(Z \to b\bar{b})/\Gamma(Z \to hadrons)$

- Impact Parameter Analysis
- Vertex Analysis
- Systematic Errors

B Lifetime

- Impact Parameter Analysis
- Vertex Analysis
- Systematic Errors

Left−Right Forward−Backward Asymmetries A_b and A_c

- Jet Charge Analysis
- Lepton Analysis

1 SLD Experiment

1.1 Luminosity and Polarization

The SLD experiment at the Stanford Linear Collider accumulated 1.8 pb^{-1} of data at the Z^0 resonance in 1993, recording a total of 50,000 hadronic Z^0 decays. This luminosity was produced by colliding electron and positron beams at an interaction point with spot size 0.8 μm by 2.4 μm. The electron beam was longitudinally polarized, with luminosity-weighted polarization $< P_e > = 0.63 \pm 0.01$.

1.2 Tracking and Calorimetry

The SLD detector is illustrated below.

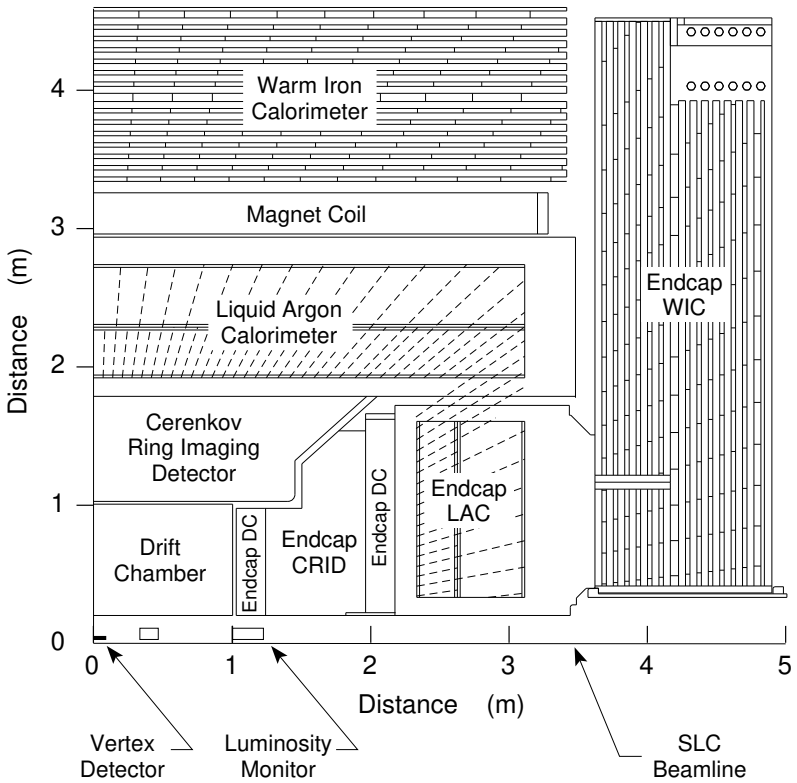

Charged particle tracking is provided by a Vertex Detector (VXD) and a Central Drift Chamber (CDC), operating in a magnetic field of 0.6 Tesla. The combined momentum resolution of the tracking system is

$$\delta p_\perp / p_\perp = \sqrt{(0.01)^2 + (0.0026\ p_\perp/\mathrm{GeV})^2}$$

in the plane perpendicular to the beam axis.

A Liquid Argon Calorimeter (LAC) measures the energies of charged and neutral particles and is also used for electron identification. The LAC is segmented into projective towers with separate electromagnetic and hadronic sections. In the barrel LAC, which covers the angular range $|\cos\theta| < 0.82$, the electromagnetic towers have transverse size $\sim$ (36 mrad)^2 and are divided longitudinally into a front section of six radiation lengths and a back section of 15 radiation lengths. The barrel LAC electromagnetic energy resolution is $\sigma_E/E = 15\%/\sqrt{E(\mathrm{GeV})}$.

Muon tracking is provided by a Warm Iron Calorimeter (WIC). The WIC is four interaction lengths thick and surrounds the $2.8+0.7$ interaction lengths of the LAC and SLD magnet coil. Sixteen layers of plastic streamer tubes interleaved with 2-in thick plates of iron absorber provide muon hit resolutions of 0.4 cm and 2.0 cm in the azimuthal and axial directions respectively.

For most of the analyses presented in this paper, events were selected by requiring at least 15 GeV of energy in the LAC and at least six tracks with $p_\perp > 0.25$ GeV in the CDC. These requirements select a sample of 37,500 hadronic Z^0 events with negligible background.

1.3 Vertex Detector

The SLD Vertex Detector is of special importance for heavy quark physics. It is a CCD pixel device with cylindrical barrel geometry, covering the angular range $|\cos\theta| < 0.74$. The detector has four layers of CCD planes, located at radii 29.5 mm to 41.5 mm from the beam line. A typical track produces hits in two or three of these layers. There are 480 CCDs in all, each containing 385×578 pixels of size 22 μm $\times$ 22 μm.

The intrinsic impact parameter resolution of the vertex detector can be measured from the apparent separation of back-to-back muons in $Z^0 \to \mu\mu$ events. A simple parametrization of the overall impact parameter resolution, including multiple scattering at low momentum, is

$$\sigma_{xy} = 11\mu\text{m} \oplus \left[\frac{70\mu\text{m}}{p \sin^{3/2}\theta}\right] \qquad \sigma_{Rz} = 38\mu\text{m} \oplus \left[\frac{70\mu\text{m}}{p \sin^{3/2}\theta}\right].$$

The small and stable SLC interaction point enables this resolution to be fully exploited. The IP is tracked using $Z^0 \to hadron$ events, providing a resolution of 6 μm in the xy-plane and 35 μm in the z direction.

2 $R_b = \Gamma(Z \to b\bar{b})/\Gamma(Z \to hadrons)$

R_b is the relative partial width of the Z^0 to $b\bar{b}$ final states, measured experimentally as the fraction of hadronic Z^0 decays containing b quarks. R_b is interesting theoretically, since it is sensitive to vertex corrections but insensitive to QCD and oblique corrections. Extensions to the Standard Model, such as extra Higgs doublets or supersymmetry, are expected to affect R_b at the 1% level.

In the SLD analysis of R_b, $Z^0 \to b\bar{b}$ events are tagged using the vertex detector. Two techniques are used—a track impact parameter analysis and a displaced vertex analysis. Both techniques rely on the small, stable SLC interaction point and the excellent vertex detector resolution to select events containing tracks originating from secondary decays of b quarks. For reference, a typical B meson decays roughly 3 mm from the IP, producing tracks with impact parameters of roughly 240 μm.

2.1 R_b Impact Parameter Analysis

The impact parameter analysis is based on signed, normalized impact parameters for tracks passing a loose set of quality cuts. The normalized impact parameter is defined as the ratio of the two-dimensional track impact parameter (distance of closest approach to the event IP in the plane normal to the beam axis) to the track impact parameter error. The impact parameter error is a convolution of the track error and the uncertainty in the IP location. The impact parameter

is signed by comparing the track direction to the direction of the nearest jet, so that a positive impact parameter corresponds to a track originating from a decay vertex in the forward jet direction.

The distribution of normalized track impact parameters is shown below. The negative tail consists mostly of fragmentation tracks and gives a measure of the detector resolution. The large positive tail is dominated by tracks originating from secondary decays of b quarks. The Monte Carlo simulation of the drift chamber + vertex detector tracking reproduces the data extremely well.

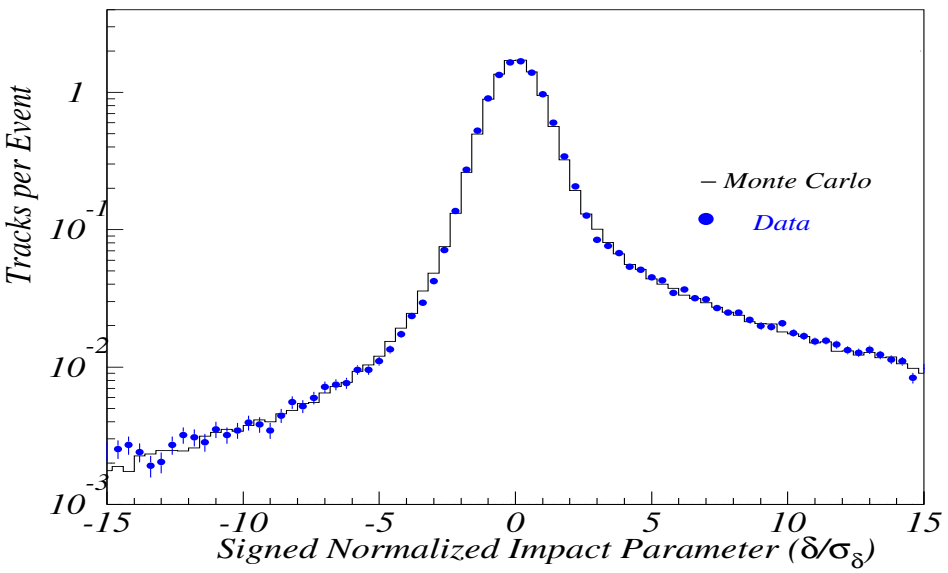

$Z^0 \to b\bar{b}$ events are tagged by requiring three or more tracks with impact parameter > 3 sigma. This tag gives an efficiency of 63% and a purity of 89%, according to the Monte Carlo simulation of Z^0 decays and detector response. R_b is extracted from the data by combining the b-tag fraction in the data with the b-tag efficiency from the Monte Carlo, after correcting for light quark contamination using the c-tag and uds-tag efficiencies from the Monte Carlo. We obtain

$$R_b = 0.230 \pm 0.005(\text{stat}) \pm 0.013(\text{syst}) \quad .$$

2.2 R_b Vertex Analysis

The vertex analysis is based on reconstructing three-dimensional vertices displaced from the IP. For this analysis, simple vertexing is sufficient; no attempt is made to resolve track-vertex ambiguities or reconstruct $b \to c$ cascade decays. Details of a more sophisticated vertex analysis will be presented later.

$Z^0 \to b\bar{b}$ events are tagged by requiring four or more vertices displaced from the IP by more than 3 sigma. This tag gives an efficiency of 73% and a purity of 79%, according to the Monte Carlo simulation of Z^0 decays and detector response. R_b is extracted as in the impact parameter analysis, by combining the b-tag fraction in the data with the b-tag efficiency from the Monte Carlo. We obtain

$$R_b = 0.219 \pm 0.005(\text{stat}) \pm 0.014(\text{syst}) \quad .$$

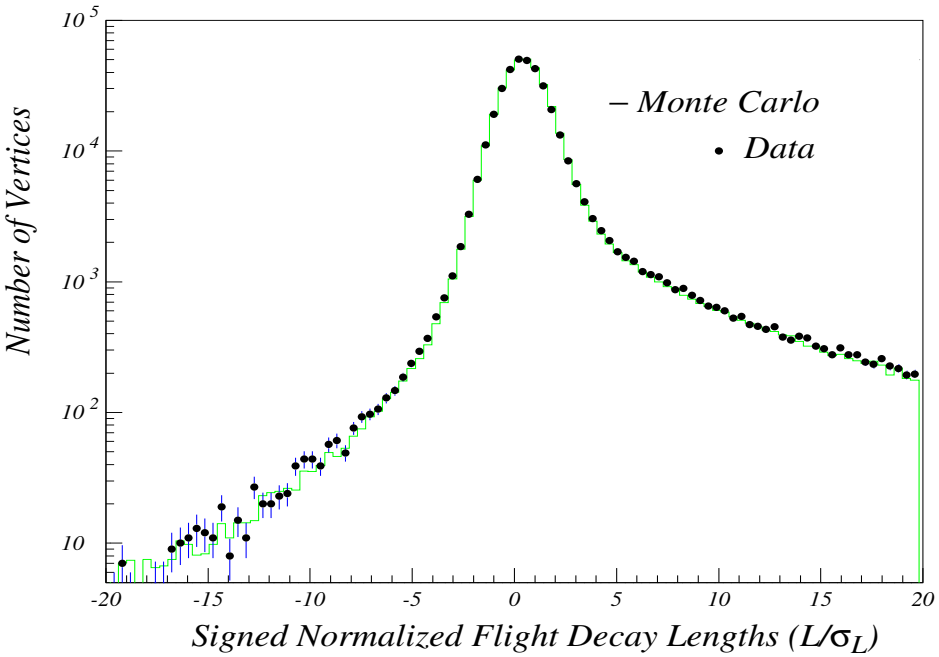

2.3 R_b Systematic Errors

Systematic errors for the two analyses are presented in the following table. The impact parameter analysis is relatively sensitive to lifetime assumptions, while the vertex analysis is more sensitive to overall track multiplicities.

R_b systematic errors	Impact $\delta R_b/R_b$	Vertex $\delta R_b/R_b$
Track multiplicity	3.0 %	4.5 %
b fragmentation	2.4 %	1.1 %
c fragmentation	0.6 %	0.2 %
B-decay multiplicity	2.4 %	3.6 %
B lifetime	2.7 %	1.2 %
$\Gamma(Z^0 \to c\bar{c})$	2.1 %	1.8 %
Overall	5.7 %	6.4 %

3 B Lifetime

SLD measurements of the B lifetime are (so far) inclusive only, averaging over the different B hadrons procuded at the Z^0. Impact parameter and vertex analyses have both been performed.

3.1 B Lifetime Impact Parameter Analysis

The B lifetime impact parameter analysis is similar to the R_b analysis. $Z^0 \to b\bar{b}$ events are selected by counting tracks with large impact parameters in a single jet. We require at least three tracks with impact parameter > 3 sigma. This yields a b-tag efficiency of 30% and a purity of 93%.

The B lifetime is then extracted from the distribution of track impact parameters in the event hemisphere opposite the tagging jet, shown below. The data is very well-reproduced by a Monte Carlo simulation of Z^0 decays in the detector, with B lifetime adjusted to match the data. This analysis yields

$$\tau_b = 1.617 \pm 0.048(\text{stat}) \pm 0.086(\text{syst}) \quad \text{ps.}$$

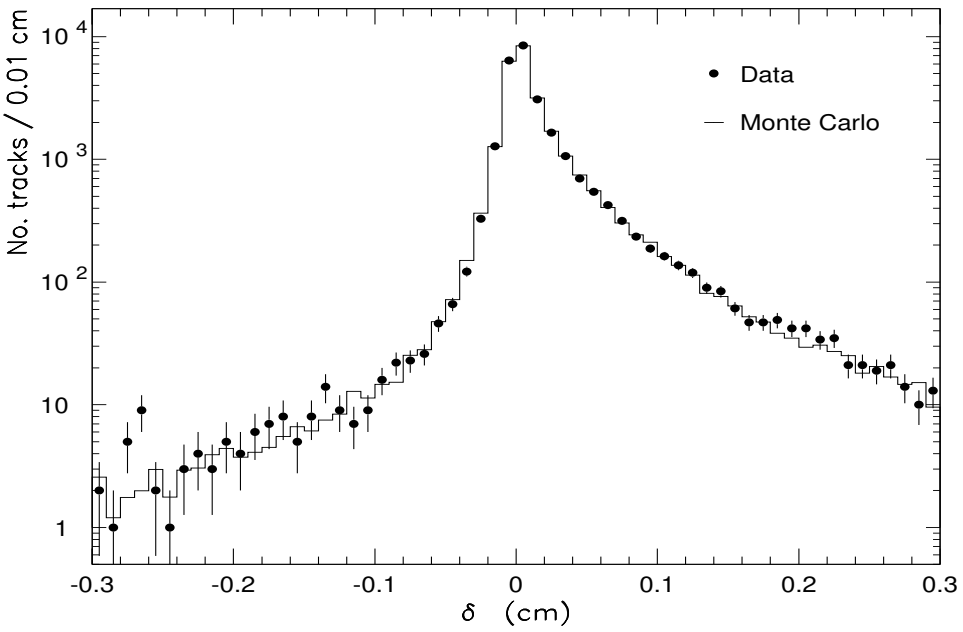

3.2 B Lifetime Vertex Analysis

The vertex analysis extracts the B lifetime directly from the measured decay lengths of a selected sample of secondary vertices. The analysis starts by tagging $Z^0 \to b\bar{b}$ events by an impact parameter tag, requiring three tracks with impact parameter > 3 sigma. Roughly 4300 events are tagged.

Geometric vertices are then reconstructed in three-dimensional from all tracks passing a loose set of quality cuts. Vertices are required to have decay length > 1 mm and at least one track inconsistent with the IP. Track sharing combinatorics produces roughly 20 such vertices per event. These vertices are then partitioned into sets where each track is used only once, and the partition with the best joint probability is selected. This reduces the vertex count to typically one to three vertices per event. In each event hemisphere, the vertex with the shortest decay length is finally kept.

The Monte Carlo simulation of Z^0 decays in the detector reproduces the data quite well, matching the distributions of vertex multiplicity, tracks/vertex, momentum, and transverse momentum. The Monte Carlo can be used to classify the final set of selected vertices according to their original quark content, as

shown in the following table. As can be seen, 88% of the selected vertices contain some B lifetime information.

Vertex track origin	Fraction
Direct b decay only	22%
$b \to c$ decay only	23%
b and $b \to c$ decays	35%
Mixed, including b or $b \to c$	8%
Direct c decay only	9%
Other mixtures	3%

For those vertices containing only tracks from direct b decay, the measured decay length reproduces the true B vertex position with a resolution of 275 μm. Vertices containing tracks from cascade $b \to c$ decay have considerably longer measured decay lengths. The B lifetime is extracted from the measured distribution of vertex decay lengths by means of a maximum likelihood comparison of the data to the Monte Carlo, shown below. We obtain

$$\tau_b = 1.577 \pm 0.032(\text{stat}) \pm 0.046(\text{syst}) \quad \text{ps}.$$

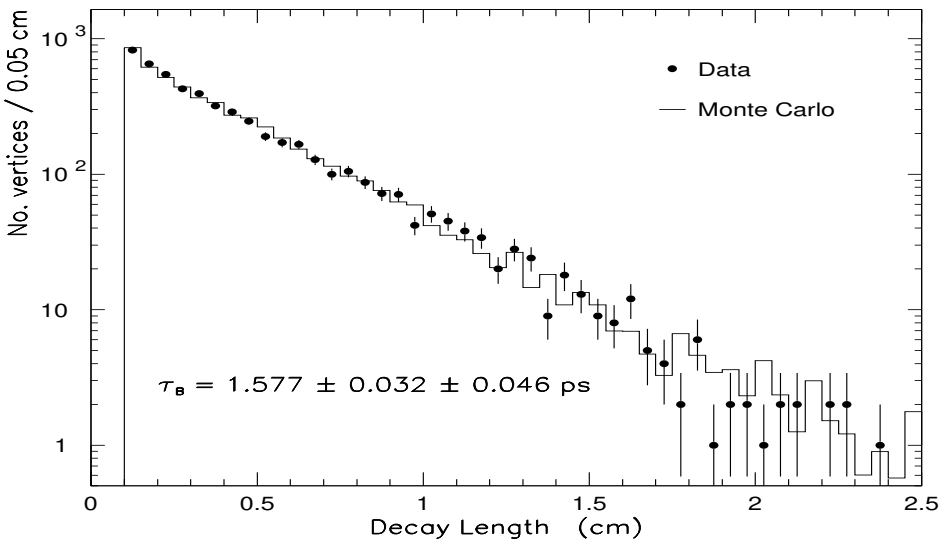

3.3 B Lifetime Systematic Errors

Systematic errors for the two B lifetime analyses are presented in the following table. The vertex analysis has clearly superseded the impact parameter analysis.

τ_b systematic errors	Impact $\delta\tau_b/\tau_b$	Vertex $\delta\tau_b/\tau_b$
Track resolution	1.4 %	——
Track efficiency	0.9 %	0.8 %
R_b and R_c	2.8 %	——
b fragmentation	2.9 %	2.4 %
c fragmentation	0.4 %	0.2 %
B multiplicity	1.9 %	0.4 %
$B \to D$ fractions	1.3 %	1.1 %
B baryon fraction	2.0 %	0.2 %
Overall	5.3 %	2.8 %

4 Left-Right Forward-Backward Asymmetry

Measurements of fermion asymmetries at the Z^0 resonance probe a combination of the vector and axial vector couplings of the Z^0 to fermions, $A_f = 2v_f a_f/(v_f^2+a_f^2)$. The parameters A_f express the extent of parity violation at the Zff vertex and provide sensitive tests of the Standard Model. The parameter A_b is particularly interesting theoretically, since it is sensitive at the 1% level to electroweak radiative corrections to the Zbb vertex but insensitive to propagator corrections which modify the weak mixing angle $\sin^2\theta_W$.

The Born-level differential cross section for the reaction $e^+e^- \to Z^0 \to f\bar{f}$ is

$$\frac{d\sigma_f}{d\cos\theta} \propto (1 - A_e P_e)(1+\cos^2\theta) + 2A_f(A_e - P_e)\cos\theta\,, \qquad (1)$$

θ = fermion direction relative to electron beam

P_e = electron beam polarization (L, R = -1, +1).

The parameter A_f can be isolated by forming the left-right forward-backward asymmetry:

$$\tilde{A}^f_{FB}(\cos\theta) = \frac{[\sigma^f_L(\cos\theta) - \sigma^f_L(-\cos\theta)] - [\sigma^f_R(\cos\theta) - \sigma^f_R(-\cos\theta)]}{[\sigma^f_L(\cos\theta) + \sigma^f_L(-\cos\theta)] + [\sigma^f_R(\cos\theta) + \sigma^f_R(-\cos\theta)]} \quad (2)$$

$$= |P_e|\, A_f \left(\frac{2\cos\theta}{1+\cos^2\theta} \right). \quad (3)$$

The analysis begins by selecting $Z^0 \to b\bar{b}$ events and determining the b and $\bar{b}$ quark directions. Two complementary techniques are used:

1. A "jet charge" analysis separates $b\bar{b}$ events into two thrust axis hemispheres, then identifies the b and $\bar{b}$ quarks by means of a momentum-weighted sum over charged tracks.

2. A lepton analysis selects events containing semileptonic b or $\bar{b}$ decays, then identifies the parent b or $\bar{b}$ quark by means of the lepton charge.

Events are then classified as "left" or "right" according to the polarization of the electron beam and "forward" or "backward" according to the direction of the b quark with respect to the electron beam. The left–right forward–backward asymmetry is formed. A_b is extracted by comparing the observed asymmetry to the theoretical prediction, using a Monte Carlo simulation to determine and correct for the analyzing power of the technique.

4.1 Jet Charge Analysis

$Z^0 \to b\bar{b}$ events are selected by requiring three tracks with impact parameter > 3 sigma, as in the R_b analysis. The event thrust axis, formed from all calorimeter energy clusters, is used as an estimate of the b and $\bar{b}$ quark directions. The jet charge is formed by summing over selected charged tracks:

$$Q_p = \Sigma\, Q_{track}\, |p \cdot T|^\kappa \; sign\; (p \cdot T), \qquad \kappa = 1/2\ .$$

A negative jet charge thus associates the b quark with the forward thrust axis direction. The distribution of jet charge in the data is well-reproduced by the Monte Carlo, as shown below.

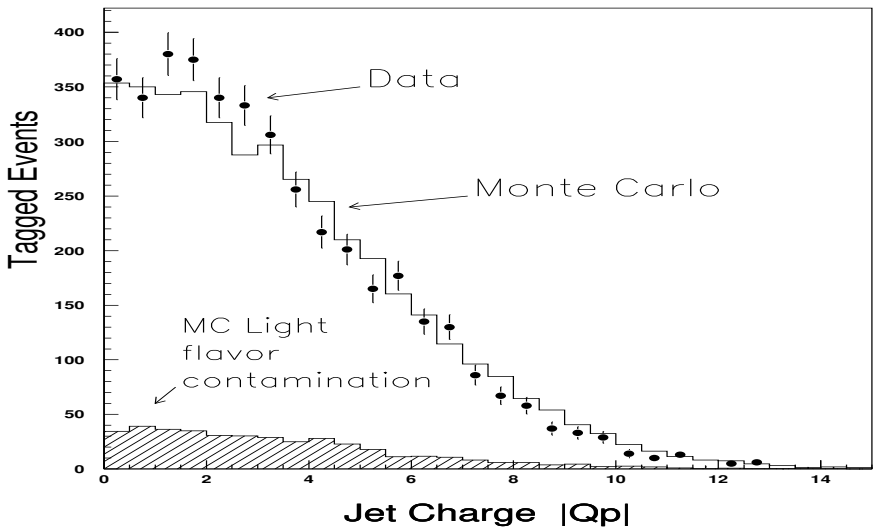

The angular distributions for L and R polarized events exhibit clear forward–backward asymmetries, even before the left–right subtraction.

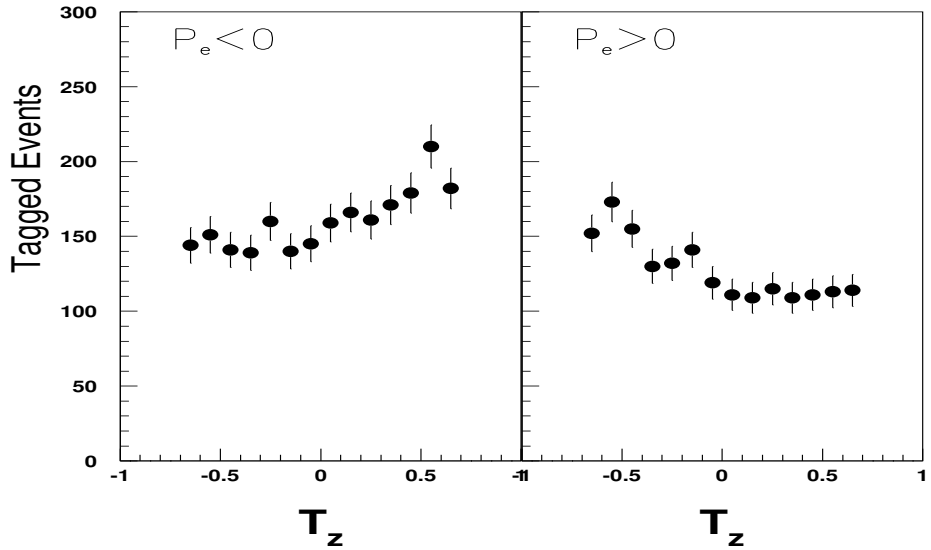

The experimental left–right forward–backward asymmetry is formed as a function of $\cos\theta$ according to Eq. (2). The sign for each event in the asymmetry sum is given by the product of the event polarization and the jet charge.

The experimental asymmetry must be corrected for various dilution effects, including the event tag purity, thrust axis smearing, and the analyzing power of the jet charge technique. These corrections are determined from the Monte Carlo simulation. The jet charge analyzing power requires the largest correction—signing the b quark correctly 70% of the time gives an analyzing power of 40%.

The parameter A_b is extracted from the corrected experimental asymmetry by fitting to the theoretical asymmetry of Eq. (3). We obtain

$$A_b = 0.93 \pm 0.13(\text{stat}) \pm 0.13(\text{syst}) \ .$$

The systematic error is dominated by the Monte Carlo model of the b-tag and the B hadron decay model.

Jet charge systematic errors	$\delta A_b/A_b$
b-tag modeling	10 %
Tracking efficiency	4 %
Thrust axis resolution	2 %
Monte Carlo statistics	5 %
B decay model	7 %
b fragmentation	2 %
$B^0 - \bar{B}^0$ mixing	1 %
Polarization	2 %
Overall	14 %

4.2 Lepton Analysis

This analysis selects $Z^0 \to b\bar{b}$ events with semileptonic b decays. Electrons are identified in the Liquid Argon Calorimeter by requiring agreement between the track momentum and the calorimeter electromagnetic energy, little or no calorimeter hadronic energy, and a reasonable front/back electromagnetic energy ratio. Muons are identified in the Warm Iron Calorimeter by comparing hits in the WIC with the extrapolated track, and taking track extrapolation errors and multiple scattering into account.

A simple analysis selects leptons with very high momentum and transverse momentum with respect to the jet axis, forms the experimental left–right forward–backward asymmetry, corrects for dilution effects, and extracts A_b. A more sophisticated analysis extracts A_b and A_c from a broader sample of leptons, using a maximum likelihood fit of the identified leptons to the theoretical cross-section.

The simple high $\{p, p_t\}$ analysis selects a clean sample of leptons from direct b decay by applying an elliptical cut on momentum and transverse momentum—$(p/18)^2 + (p_t/1.1)^2 > 1$ for muons and $(p/14)^2 + (p_t/1.0)^2 > 1$ for electrons. Roughly half of all leptons from direct b decay pass these high $\{p, p_t\}$ cuts. The selected lepton sample, consisting of 613 electrons and 576 muons, is 70% pure (direct b decay).

The experimental left–right forward–backward asymmetry is formed as a function of $\cos\theta$ according to Eq. (2). The sign for each event in the asymmetry sum is given by the product of the event polarization and the b quark direction, which in turn is given by the jet direction and the lepton charge. The observed asymmetry is shown below.

The Monte Carlo is used to estimate the composition of the lepton sample, determining the contributions to the observed asymmetry from all lepton sources and backgrounds.

Lepton source	Asymmetry	μ fraction	e fraction
$b \to l$	$(1-2\chi)A_b$	73%	69%
$b \to c \to \bar{l}$	$-(1-2\chi)A_b$	6%	7%
$b \to \bar{c} \to l$	$(1-2\chi)A_b$	1%	1%
$c \to l$	$-A_c$	7%	8%
Hadron $\to l$	A_{bkg}	2%	2%
Misidentified l	A_{bkg}	11%	13%

The maximum likelihood analysis replaces the hard lepton $\{p, p_t\}$ cut and subsequent Monte Carlo categorization of lepton sources with an event-by-event, momentum dependent estimate of the lepton source probabilities. This analysis gives a result consistent with the simple high $\{p, p_t\}$ analysis and is used for the final determination of A_b and A_c.

The likelihood function contains the following probability term for each lepton in the data:

$$P\left(p, p_t,\, P_e, Q, \cos\theta;\, A_b, A_c\right) \;\propto\; 1 \,+\, \left(\frac{A_e - P_e}{1 - A_e P_e}\right)\left(\frac{-2Q\cos\theta}{1+\cos^2\theta}\right)$$
$$\times \left\{\, f_b\,(1-2\chi)\,[1+\Delta^b_{QCD}(\cos\theta)]\,A_b \;-\; f_c\,[1+\Delta^c_{QCD}(\cos\theta)]\,A_c \;+\; f_{bkg}\,A_{bkg} \,\right\}.$$

The three signs governing the asymmetry—beam polarization P_e, lepton charge Q, and jet direction $\cos\theta$—are incorporated automatically into the maximum likelihood probability function. The lepton source fractions (f_b, f_c, f_{bkg}) are derived by counting leptons in the MC with similar p and p_t to each lepton in the data. The f_b term combines direct and cascade b-quark decays, signed according to their asymmetry contributions. A correction factor $(1-2\chi)$ is applied to all b-quark lepton sources to account for asymmetry dilution due to $B^0\bar{B}^0$ mixing, with $\chi = 0.12$ taken from LEP measurements of the average mixing in $Z^0 \to b\bar{b}$ events. The background asymmetry A_{bkg} is derived as a function of p and p_t from tracks in the data not identified as leptons. A QCD correction factor is applied to the theoretical asymmetry function to incorporate known QCD corrections to the cross section. The QCD correction is as large as 5% at $\cos\theta = 0$ and its inclusion decreases the asymmetry by 3% overall.

The final maximum likelihood results are as follows:

muons: $A_b = 0.94 \pm 0.20(\text{stat}) \pm 0.10(\text{syst})$

$A_c = 0.42 \pm 0.29(\text{stat}) \pm 0.18(\text{syst})$

electrons: $A_b = 0.92 \pm 0.19(\text{stat}) \pm 0.12(\text{syst})$

$A_c = 0.37 \pm 0.37(\text{stat}) \pm 0.31(\text{syst})$

combined: $A_b = 0.93 \pm 0.14(\text{stat}) \pm 0.09(\text{syst})$

$A_c = 0.40 \pm 0.23(\text{stat}) \pm 0.20(\text{syst}).$

Systematic errors have been estimated for a number of sources, summarized in the following table.

Source	$\delta A_b(\mu)$	$\delta A_b(e)$	$\delta A_c(\mu)$	$\delta A_c(e)$
Monte Carlo weights	0.04	0.08	0.08	0.18
Track efficiency	0.01	0.02	0.01	0.01
Jet axis simulation	0.06	0.04	0.06	0.13
Background level	0.02	0.01	0.03	0.01
Background asymmetry	0.01	0.01	0.03	0.09
BR($Z^0 \to b\bar{b}$)	0.01	0.00	0.00	0.00
BR($Z^0 \to c\bar{c}$)	0.01	0.00	0.03	0.03
$B^{\pm}, B^0$ lepton spectrum	0.02	0.05	0.12	0.14
B_s lepton spectrum	0.03	0.02	0.05	0.05
Λ_b lepton spectrum	0.01	0.01	0.02	0.03
D lepton spectrum	0.02	0.02	0.04	0.10
Polarization	0.02	0.02	0.01	0.01
Second order QCD	0.01	0.01	0.04	0.04
B mixing χ	0.03	0.03	0.00	0.00
Total	0.10	0.12	0.18	0.31

† SLD Collaboration:

K. Abe,[29] I. Abt,[14] C. J. Ahn,[26] T. Akagi,[27] W. W. Ash,[27] D. Aston,[27]
N. Bacchetta,[21] K. G. Baird,[24] C. Baltay,[33] H. R. Band,[32]
M. B. Barakat,[33] G. Baranko,[10] O. Bardon,[16] T. Barklow,[27]
A. O. Bazarko,[11] R. Ben-David,[33] A. C. Benvenuti,[2] T. Bienz,[27]
G. M. Bilei,[22] D. Bisello,[21] G. Blaylock,[7] J. R. Bogart,[27] T. Bolton,[11]
G. R. Bower,[27] J. E. Brau,[20] M. Breidenbach,[27] W. M. Bugg,[28]
D. Burke,[27] T. H. Burnett,[31] P. N. Burrows,[16] W. Busza,[16]
A. Calcaterra,[13] D. O. Caldwell,[6] D. Calloway,[27] B. Camanzi,[12]
M. Carpinelli,[23] R. Cassell,[27] R. Castaldi,[23] A. Castro,[21]
M. Cavalli-Sforza,[7] E. Church,[31] H. O. Cohn,[28] J. A. Coller,[3] V. Cook,[31]
R. Cotton,[4] R. F. Cowan,[16] D. G. Coyne,[7] A. D'Oliveira,[8]
C. J. S. Damerell,[25] S. Dasu,[27] R. De Sangro,[13] P. De Simone,[13]
R. Dell'Orso,[23] M. Dima,[9] P. Y. C. Du,[28] R. Dubois,[27] B. I. Eisenstein,[14]
R. Elia,[27] D. Falciai,[22] C. Fan,[10] M. J. Fero,[16] R. Frey,[20] K. Furuno,[20]
T. Gillman,[25] G. Gladding,[14] S. Gonzalez,[16] G. D. Hallewell,[27]
E. L. Hart,[28] Y. Hasegawa,[29] S. Hedges,[4] S. S. Hertzbach,[17]
M. D. Hildreth,[27] J. Huber,[20] M. E. Huffer,[27] E. W. Hughes,[27]
H. Hwang,[20] Y. Iwasaki,[29] P. Jacques,[24] J. Jaros,[27] A. S. Johnson,[3]
J. R. Johnson,[32] R. A. Johnson,[8] T. Junk,[27] R. Kajikawa,[19] M. Kalelkar,[24]
I. Karliner,[14] H. Kawahara,[27] H. W. Kendall,[16] Y. Kim,[26] M. E. King,[27]
R. King,[27] R. R. Kofler,[17] N. M. Krishna,[10] R. S. Kroeger,[18] J. F. Labs,[27]
M. Langston,[20] A. Lath,[16] J. A. Lauber,[10] D. W. G. Leith,[27] X. Liu,[7]
M. Loreti,[21] A. Lu,[6] H. L. Lynch,[27] J. Ma,[31] G. Mancinelli,[22] S. Manly,[33]
G. Mantovani,[22] T. W. Markiewicz,[27] T. Maruyama,[27] R. Massetti,[22]
H. Masuda,[27] E. Mazzucato,[12] A. K. McKemey,[4] B. T. Meadows,[8]
R. Messner,[27] P. M. Mockett,[31] K. C. Moffeit,[27] B. Mours,[27] G. Müller,[27]
D. Muller,[27] T. Nagamine,[27] U. Nauenberg,[10] H. Neal,[27] M. Nussbaum,[8]
Y. Ohnishi,[19] L. S. Osborne,[16] R. S. Panvini,[30] H. Park,[20] T. J. Pavel,[27]
I. Peruzzi,[13] L. Pescara,[21] M. Piccolo,[13] L. Piemontese,[12] E. Pieroni,[23]
K. T. Pitts,[20] R. J. Plano,[24] R. Prepost,[32] C. Y. Prescott,[27]
G. D. Punkar,[27] J. Quigley,[16] B. N. Ratcliff,[27] T. W. Reeves,[30]
P. E. Rensing,[27] L. S. Rochester,[27] J. E. Rothberg,[31] P. C. Rowson,[11]
J. J. Russell,[27] O. H. Saxton,[27] T. Schalk,[7] R. H. Schindler,[27]

U. Schneekloth,[16] B. A. Schumm,[15] A. Seiden,[7] S. Sen,[33] V. V. Serbo,[32]
M. H. Shaevitz,[11] J. T. Shank,[3] G. Shapiro,[15] S. L. Shapiro,[27]
D. J. Sherden,[27] C. Simopoulos,[27] N. B. Sinev,[20] S. R. Smith,[27]
J. A. Snyder,[33] P. Stamer,[24] H. Steiner,[15] R. Steiner,[1] M. G. Strauss,[17]
D. Su,[27] F. Suekane,[29] A. Sugiyama,[19] S. Suzuki,[19] M. Swartz,[27]
A. Szumilo,[31] T. Takahashi,[27] F. E. Taylor,[16] E. Torrence,[16] J. D. Turk,[33]
T. Usher,[27] J. Va'vra,[27] C. Vannini,[23] E. Vella,[27] J. P. Venuti,[30]
P. G. Verdini,[23] S. R. Wagner,[27] A. P. Waite,[27] S. J. Watts,[4]
A. W. Weidemann,[28] J. S. Whitaker,[3] S. L. White,[28] F. J. Wickens,[25]
D. A. Williams,[7] D. C. Williams,[16] S. H. Williams,[27] S. Willocq,[33]
R. J. Wilson,[9] W. J. Wisniewski,[5] M. Woods,[27] G. B. Word,[24] J. Wyss,[21]
R. K. Yamamoto,[16] J. M. Yamartino,[16] X. Yang,[20] S. J. Yellin,[6]
C. C. Young,[27] H. Yuta,[29] G. Zapalac,[32] R. W. Zdarko,[27] C. Zeitlin,[20]
and J. Zhou.[20]

[1]Adelphi University, Garden City, New York 11530, U.S.A.
[2]INFN Sezione di Bologna, I-40126 Bologna, Italy.
[3]Boston University, Boston, Massachusetts 02215, U.S.A.
[4]Brunel University, Uxbridge, Middlesex UB8 3PH, United Kingdom.
[5]California Institute of Technology, Pasadena, California 91125, U.S.A.
[6]University of California at Santa Barbara, Santa Barbara, California 93106, U.S.A.
[7]University of California at Santa Cruz, Santa Cruz, California 95064, U.S.A.
[8]University of Cincinnati, Cincinnati, Ohio 45221, U.S.A.
[9]Colorado State University, Fort Collins, Colorado 80523, U.S.A.
[10]University of Colorado, Boulder, Colorado 80309, U.S.A.
[11]Columbia University, New York, New York 10027, U.S.A.
[12]INFN Sezione di Ferrara and Università di Ferrara, I-44100 Ferrara, Italy.
[13]INFN Lab. Nazionali di Frascati, I-00044 Frascati, Italy.
[14]University of Illinois, Urbana, Illinois 61801, U.S.A.
[15]Lawrence Berkeley Laboratory, University of California, Berkeley, California 94720, U.S.A.
[16]Massachusetts Institute of Technology, Cambridge, Massachusetts 02139, U.S.A.
[17]University of Massachusetts, Amherst, Massachusetts 01003, U.S.A.
[18]University of Mississippi, University, Mississippi 38677, U.S.A.
[19]Nagoya University, Chikusa-ku, Nagoya 464, Japan.
[20]University of Oregon, Eugene, Oregon 97403, U.S.A.

[21]INFN Sezione di Padova and Università di Padova, I-35100 Padova, Italy.
[22]INFN Sezione di Perugia and Università di Perugia, I-06100 Perugia, Italy.
[23]INFN Sezione di Pisa and Università di Pisa, I-56100 Pisa, Italy.
[24]Rutgers University, Piscataway, New Jersey 08855, U.S.A.
[25]Rutherford Appleton Laboratory, Chilton, Didcot, Oxon OX11 0QX United Kingdom.
[26]Sogang University, Seoul, Korea.
[27]Stanford Linear Accelerator Center, Stanford University, Stanford, California 94309, U.S.A.
[28]University of Tennessee, Knoxville, Tennessee 37996, U.S.A.
[29]Tohoku University, Sendai 980 Japan.
[30]Vanderbilt University, Nashville, Tennessee 37235, U.S.A.
[31]University of Washington, Seattle, Washington 98195, U.S.A.
[32]University of Wisconsin, Madison, Wisconsin 53706, U.S.A.
[33]Yale University, New Haven, Connecticut 06511, U.S.A.